Propagation of a plasma streamer in catalyst pores

Propagation of a plasma streamer in catalyst pores

Quan-Zhi Zhang*, and Annemie Bogaerts*

Research Group PLASMANT, University of Antwerp, Universiteitsplein 1, B-2610 Antwerp-Wilrijk, Belgium

*Corresponding author.

Email: Quan-Zhi.Zhang@uantwerpen.be (Q.Z. Zhang), annemie.bogaerts@uantwerpen.be (A. Bogaerts).

Abstract

Although plasma catalysis is gaining increasing interest for various environmental applications, the underlying mechanisms are still far from understood. For instance, it is not yet clear whether and how plasma streamers can propagate in catalyst pores, and what is the minimum pore size to make this happen. As this is crucial information to ensure good plasma-catalyst interaction, we study here the mechanism of plasma streamer propagation in a catalyst pore, by means of a two-dimensional particle-in-cell/Monte Carlo collision model, for various pore diameters in the nm-range to μm-range. The so-called Debye length is an important criterion for plasma penetration into catalyst pores, i.e., a plasma streamer can penetrate into pores when their diameter is larger than the Debye length. The Debye length is typically in the order of a few 100 nm up to 1 μm at the conditions under study, depending on electron density and temperature in the plasma streamer. For pores in the range of ~ 50 nm, plasma can thus only penetrate to some extent and at very short times, i.e., at the beginning of a micro-discharge, before the actual plasma streamer reaches the catalyst surface and a sheath is formed in front of the surface. We can make plasma streamers penetrate into smaller pores (down to ca. 500 nm at the conditions under study) by increasing the applied voltage, which yields a higher plasma density, and thus reduces the Debye length. Our simulations also reveal that the plasma streamers induce surface charging of the catalyst pore sidewalls, causing discharge enhancement inside the pore, depending on pore diameter and depth.

Keywords: Plasma streamer; Catalyst pores; PIC/MCC simulation; Plasma catalysis; Micro-discharge

1. Introduction

Plasma catalysis is becoming a rapidly growing research area for environmental applications, such as air pollution control, hydrocarbon reforming, greenhouse gas conversion, and nitrogen fixation [1-7]. Plasma is a (partially) ionized gas, consisting of energetic electrons, ions, radicals, excited species, besides neutral gas molecules. The energetic electrons can induce thermodynamically difficult reactions at room temperatures. Due to its high reactivity, plasma reactions are, however, not very selective. To improve the product selectivity, catalytically active packing material (e.g. beads or pellets) can be inserted in the discharge. Thus, plasma catalysis combines the advantages of both catalysis (selectivity) and plasma technology (high reactivity), and often yields synergistic effects [1-7]. However, the underlying mechanisms of plasma catalysis are far from understood, due to the complicated interactions between catalyst and plasma.

On one hand, exposing the catalyst to the abundant reactive plasma species affects its morphology or work function [1]. On the other hand, the presence of a catalyst in the plasma zone influences the discharge characteristics, among others by enhancing the electric field near the packing beads or pellets [8]. In addition, numerous micro-discharges can be created between the catalytic beads or pellets. These micro-discharges will charge the catalytic materials, and induce surface discharges, which will lead to a higher concentration of reactive species around the catalyst [9]. Furthermore, micro-

discharges may be formed inside the catalyst pores (including inter-particle pores at the contact points between the beads or pellets, and intra-particle pores inside the beads or pellets). This is of crucial importance for plasma catalysis, as it defines the catalyst surface area exposed to the plasma species, and thus the ultimate performance of plasma catalysis [10–13].

Holzer et al. tried to obtain a better understanding of the micro-discharge properties inside catalyst pores, and studied the accessibility of intra-particle pores (with size in the mesoporous range, i.e., tens of nm) for short-lived oxidizing plasma species, by investigating the oxidation of organic compounds immobilized on porous and non-porous alumina and silica [10]. They provided the first experimental evidence for the presence of reactive plasma species in the inner volume of porous catalysts with typical pore size of 10 nm. Furthermore, they demonstrated that the reaction selectivity of hydrocarbon oxidation to CO_2 is significantly higher in case of a porous catalyst in the discharge zone than with a non-porous catalyst. The short-lived plasma species inside the pores are believed to play a very important role in the reaction selectivity. Holzer et al. speculated that these radicals mainly diffuse into the pores from the plasma and are not directly formed in the pores, but the actual generation mechanisms are not yet clarified [10]. The same group further reported that porous catalysts can provide wider oxidation pathways of volatile organic model compounds [11], and again they suggested the presence of plasma in the interior of catalyst pores, by means of electron paramagnetic resonance, demonstrating the formation of paramagnetic species in the absence of gas-phase oxygen with a porous Al_2O_3 catalyst, which were not observed in non-porous Al_2O_3 [12]. However, as the actual generation mechanisms are not yet clarified, it is a crucial research question to understand the underlying plasma behavior in a catalyst pore with size of tens of nm.

Furthermore, Hensel et al. studied the discharge pattern for porous ceramic materials in atmospheric air [13]. The authors demonstrated that the discharge only developed along the dielectric surface for small pores of 0.8 μm, i.e., so-called surface discharges. When increasing the pore size to 15 μm, the surface discharge could leak into the ceramic pores, and a transition of discharge mode from surface discharge to micro-discharge was observed. This indicated that the formation of micro-discharges is very sensitive to the pore size. Subsequently, the same group investigated the micro-discharge characteristics for various pore sizes, discharge powers, and gas mixtures [14]. They demonstrated that the onset voltage to create micro-discharges inside catalyst pores increases with decreasing pore size. Thus, both pore size and applied voltage are critical parameters for micro-discharge formation in porous materials [15].

The above experimental studies, although very interesting, could only provide general results, with limited insights in the underlying mechanisms, and thus, the inherent mechanisms behind micro-discharge formation in catalyst pores are still poorly understood. Recently, Zhang et al. developed a two-dimensional (2D) fluid model to study the formation mechanism of micro-discharges in inter-particle macro (10 ~ 400 μm) pores, for a plasma operating in glow discharge mode in helium [16-17]. The authors pointed out that the plasma species can only be generated inside pores in the μm range (≥30 μm) due to the limitation of the Debye length (which is indeed in the μm range for a helium plasma in glow discharge mode). However, most applications of plasma catalysis are based on reactive gases instead of helium, like air, CO_2, hydrocarbons and their mixtures, in which the plasma can behave very differently and the plasma density can be much higher due to streamer formation. This can induce a much smaller Debye length and enable the plasma to penetrate into smaller catalyst pores. Zhang et al. later investigated the micro-discharge characteristics in nm-sized catalyst pores by means of a 2D particle-in cell/Monte Carlo collision (PIC/MCC) model [18], but they applied some general plasma properties in the streamer head (as

obtained from other simulations) as the initial boundary condition of their model, which can make the plasma behave quite differently from a real streamer, as will be revealed from our results presented below.

In the present paper, we therefore investigate in detail the micro-discharge formation and the propagation of a plasma streamer in pores with different diameter and depth, as well as for different applied voltages (defining the Debye length). For this purpose, we use a 2D implicit PIC/MCC model. The calculations are performed in a dielectric barrier discharge (DBD), sustained by a DC applied voltage source and operating in air at atmospheric pressure, which is characterized by plasma streamer formation. The aim of the paper is to answer the important research question whether plasma streamers can propagate into catalyst pores, and for which pore diameters, and to reveal the mechanism of discharge enhancement inside catalyst pores.

2. Computational Model and Conditions

The simulated cylindrical discharge geometry is schematically illustrated in figure 1. It is 50 μm in height, and 37.5 or 90 μm in radius (see below). The discharge is formed in the gap between two electrodes, covered by dielectric plates with thickness of 5 μm (bottom) and 7.5 μm (top) and relative permittivity, ε_γ=4. A negative DC voltage is applied to the bottom electrode, while the top electrode is grounded. As shown in figure 1, a small pore is present in the top dielectric. The streamer is initiated by artificially placing 20 seed electrons, 20 O_2^-, 20 O_2^+, and 20 N_2^+ ions right above the bottom dielectric (z between [5 μm, 5.01 μm], r between [14.7 μm, 14.8 μm], see figure 1). Their initial velocities are sampled from a Maxwellian distribution with average energy of 2 eV for the electrons and 0.026 eV for the ions. Their initial weight ω_p is 1 (i.e., 1 super particle corresponds to 1 electron or ion), but it will automatically increase with the streamer evolution by the particle merging algorithm (explained below). Typically, the weights increase up to 10^6 for both electrons and ions, when the streamer has arrived at the top dielectric. The electrons and ions, when arriving at the dielectric, will accumulate on the dielectric surface and thus contribute to surface charging of the adjacent grids on the dielectric surface.

For charge deposition on the dielectric, as well as on the pore bottom, the charge $q_{i,j}$, at the location of (r_p, z_p), is assigned to the two adjacent grid points in the R direction, i.e. (r_i, z_i) and (r_{i+1}, z_j), as we use cylindrical coordinates in the model. The real particle number $N_{i,j}$, $N_{i+1,j}$ assigned to the grid point at (r_i, z_j) and (r_{i+1}, z_j) can be written as

$$N_{i,j} = \omega_p \frac{r_{i+1}^2 - r_p^2}{r_{i+1}^2 - r_i^2}$$
$$N_{i+1,j} = \omega_p \frac{r_p^2 - r_i^2}{r_{i+1}^2 - r_i^2}.$$

Likewise, for charge deposition on the pore sidewalls, the charge $q_{i,j}$, at the location of (r_p, z_p), is assigned to the two grid points in the Z direction, i.e. (r_i, z_i) and (r_i, z_{j+1}), and the real particle number $N_{i,j}$, $N_{i,j+1}$ assigned to the grid point at (r_i, z_j) and (r_i, z_{j+1}) can be written as

$$N_{i,j} = \omega_p \frac{z_{j+1} - z_p}{z_{j+1} - z_j}$$
$$N_{i,j+1} = \omega_p \frac{z_p - z_{j+1}}{z_{j+1} - z_j}.$$

The deposited surface charges are then converted to a volume charge density, and taken into account in the solution of the Poisson equation to self-consistently calculate the electric field distribution, including the effect of surface charging.

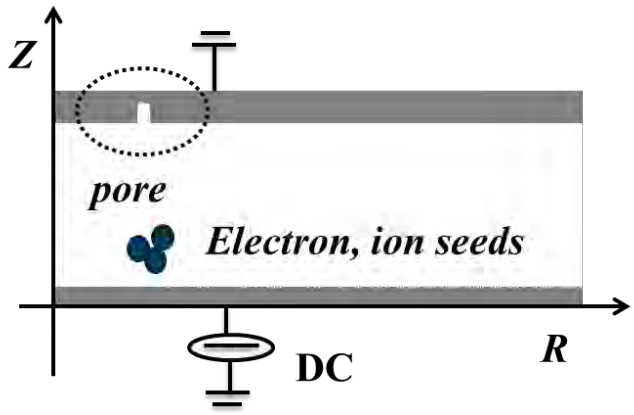

Figure 1. Schematic of the simulation geometry.

We make use of a two-dimensional implicit PIC/MCC model, and a detailed description about this model can be found in [19-20]. We use square cells in the model. To simulate the geometry with a 50 nm diameter meso-pore, the simulation region is uniformly divided into 2049 × 1500 cells (i.e. 50 μm × 37.5 μm), with a mesh size around 25 nm. This number of cells is limited by the computation time and computer memory (see below). In addition, we have also simulated a wider region, where the whole geometry is divided into 1025 × 1800 cells (i.e. 50 μm × 90 μm), yielding a mesh size of around 50 nm. The simulation time-step is fixed at 10^{-14} s, and the total simulation time ranges till 20.8 ps, which is enough to allow the plasma streamer to arrive at the top dielectric and penetrate till the bottom of the catalyst pore. Note that we simply assume a pore in a dielectric material (SiO_2 in this case, with ε_γ=4); hence not a real catalytic material, but rather a catalytic support material. Likewise, catalytic surface reactions are not included in our model, which is beyond the scope of this work. The aim of this paper is to reveal whether and how the plasma streamer penetrates into pores, and for this purpose, the pore diameter and depth, as well as the plasma conditions (gas pressure and temperature, gas mixture, and applied voltage) are most important.

We assume atmospheric air as the discharge gas, with a constant density of background molecules (O_2, N_2) at 300K. We trace free electrons, N_2^+, O_2^+ and O_2^- during the whole simulation. The reactions taken into account are elastic collisions, excitation, ionization and attachment collisions of electrons with N_2 and O_2 gas molecules, as explained in more detail in [18]. All the electron impact cross sections are taken from the lxcat database [21]. A widely used stochastic version of Zhelenyak's photoionization model [22-26] is introduced to account for photoionization, i.e. ionization of O_2 molecules after absorbing photons with a wavelength between 98 and 102.5nm, emitted by excited N_2 molecules. The number of photoionization events is calculated directly from this model, which is originally built based on experimental measurements. Note that the number of photons is not involved in this model. Good agreement has been achieved between this model and experimental measurement in [22]. This model is also widely employed in other PIC/MCC simulations [23-26]. The initial weight of new generated particles by photoionization is always equal to 1.

Since the number of electrons and ions will rapidly increase due to the ionization avalanches after a certain time, we need to introduce a particle merging algorithm to limit the computation time. We employ a 'three-two' merging algorithm [27] to restrict the particle number: when the number of super-electrons or super-ions exceeds 40 in each grid, three particles are combined into two particles with both conservation of momentum and energy.

Because we use silica as the dielectric material, which is a perfect isolator, and the applied electric field is in the same direction as the catalyst pore, we don't consider field emission in this model.

3. Results and discussion

In section 3.1, we present the evolution of a plasma streamer from a few seed electrons, and we illustrate the interaction of this plasma streamer with a mesoporous catalyst pore of 50 nm. In section 3.2, we examine the propagation of a plasma streamer inside meso-macro pores (400 nm ~ 3 μm), as well as the effect of applied voltage. To reveal the underlying mechanism of discharge enhancement inside catalyst pores, we demonstrate in section 3.3 that surface charging of the dielectric surface plays an important role in the interaction between plasma streamer and catalyst pore. Finally, in section 3.4, we study the influence of pore depth on the discharge enhancement.

3.1 Propagation of a plasma streamer in a meso-pore of 50 nm diameter

Figure 2 shows the plasma density distributions at three different times, to illustrate the evolution of a plasma streamer inside the discharge and the catalyst pore as a function of time. As seen in figure 2(a), the plasma streamer develops from the avalanche of the particle seeds after a certain distance of around 17 μm. A certain number of electrons can diffuse into the 50 nm diameter pore, which can be observed more clearly in the enlarged figure 2(d). When the streamer reaches the dielectric at 14.4 ps, the plasma density in the streamer head (right below the dielectric) becomes very high, i.e. 6.8×10^{21} m^{-3}, as shown in figure 2 (b) and (e). Some electrons can still penetrate into the pore at this moment in time. However, the high electron density in the streamer head rapidly charges the dielectric, which induces a sheath in front of the dielectric at 17.6 ps, as indicated in figure 2 (c) and (f). The plasma bulk is pushed away by the strong sheath potential, and the electron density becomes very low near the dielectric. Therefore, there is no plasma penetration into the catalyst pore anymore.

Thus, a limited number of electrons can diffuse into the catalyst pore, corresponding to a density in the order of 10^{19} m^{-3}, which is two orders of magnitude smaller than the density in the streamer head, before a sheath is generated in front of the pore. The electrons inside the pore arrive there initially by diffusion from the streamer head. However, there also exists a strong electric field in the pore, so in addition they will move by migration. The electron temperature becomes ca. 32 eV in the streamer head, which is high enough to create reactive species by electron impact collisions. The latter corresponds to the experimental data of [10, 12], where it was reported that short lived reactive species exist inside pores with nm-sized dimensions. The fact that reactive species are present inside the pores may significantly increase the effective surface area of the catalyst exposed to the plasma species, and thus enhance the catalytic reactions. However, the concentration of electrons and reactive species inside these small pores is limited by the formation time of a sheath in front of the pores. For the conditions investigated here, the sheath formation time is around 16 ps for an applied voltage of -3 kV, 14.8 ps for -5 kV, and 10 ps for -8 kV. Note that we only have 3 grid points inside the 50 nm pore. This number is limited by the computation time and computer memory. Indeed, a smaller mesh size yielded too many grid points in the entire geometry, exceeding the

memory. We also tried to reduce the entire geometry (and thus the total number of grid points) to allow a smaller mesh size in the pore, but in this way we could not evaluate a realistic streamer propagation. However, we did check our results for a 50 nm pore with those for a 200 nm diameter pore, thus having more meshes in the pore, and they showed the same behavior, as it should be, because in both cases the diameter is much smaller than the Debye length of 510 nm (see below)

We can conclude that the plasma density distribution in the streamer and the sheath formation in front of the pores play an important role in determining whether plasma can penetrate inside small intra-particle pores of a catalyst. It should be noted that these two effects were ignored to a certain degree in the model by Zhang et al. [18], because they assumed as initial conditions a continuous electron current and a very small simulation region of 1 μm × 0.3 μm (i.e., much smaller than the streamer width in figure 2 (a,b,c)). This continuous electron current cannot give a realistic streamer density distribution, and the sheath formation cannot be properly accounted for in such a small region. Thus, our model provides more insights in the underlying mechanisms.

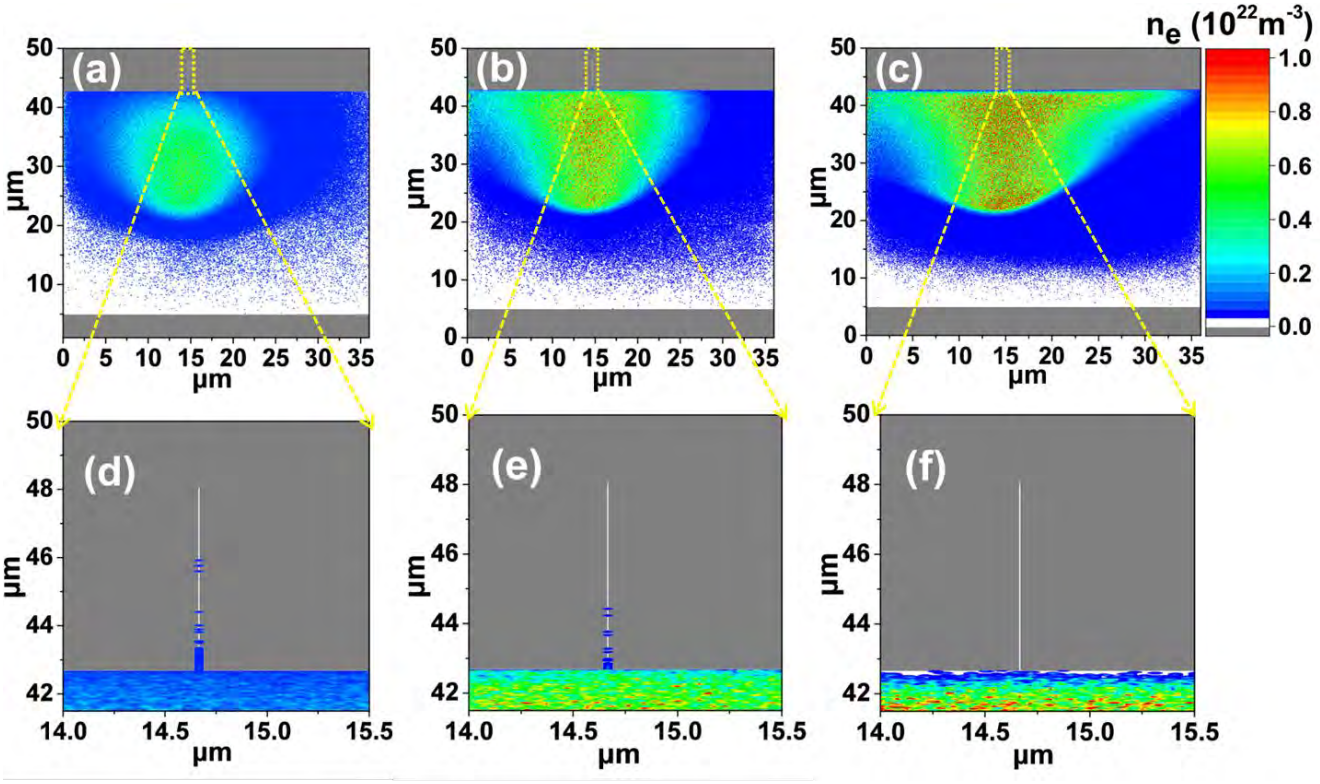

Figure 2. Plasma density distributions n_e (m^{-3}) , illustrating the evolution of a plasma streamer inside the discharge (a,b,c) and enlarged figures near the catalyst pore in the top dielectric (d,e,f), at 12.8 ps (a, d), 14.4 ps (b, e), and 17.6 ps (c, f), for an applied DC voltage of -5 kV. The pore has a diameter of 50 nm.

It is worth to mention that we can only use a very small discharge gap of 37.5 μm, due to computational limits, as defined by the number of mesh points in the simulation region. However, the space between catalytic beads or pellets in plasma catalysis can be in the order of hundreds of μm, and this can induce a much longer propagation time, in the order of 100 ps, before the plasma streamer arrives at the dielectric/catalytic surface. In that case, more electrons will be able to diffuse into the catalyst pores before a sheath is formed, thus we may expect that more reactive plasma species can then be formed inside the pores.

3.2 Effect of pore diameter and applied voltage on the plasma streamer propagation

Figure 3 illustrates the plasma density distributions near and inside a pore, for different pore diameters, at an applied DC voltage of – 3 kV at the bottom electrode. The pore depth is fixed at 5 μm. The result is plotted at 20.8 ps to allow the plasma streamer to arrive at the top dielectric and penetrate till the bottom of the catalyst pore. Note that the sheath is formed in this case at around 16 ps. A clear discharge enhancement is observed inside the pores for diameters larger than 700 nm. The strongest discharge enhancement happens in the pore with 1 μm diameter. Indeed, when the streamer arrives at the dielectric, the average plasma density n_e in the streamer head is around 3.5×10^{21} m^{-3}, and the electron temperature T_e is around 28 eV, which yields a Debye length, $\lambda_{de} \approx 7430\sqrt{T_e/n_e}$, around 670 nm. Here, T_e is in eV and n_e is in m^{-3}. Thus, the plasma can penetrate into pores with diameter larger than 800 nm (figure 3(a-c)), and give rise to discharge enhancement (see below for the mechanism). When the pore diameter is smaller than 800 nm, plasma penetration into the pores becomes difficult, and only a few electrons can be observed inside a pore with 400 nm diameter (figure 3(f)). The strongest discharge enhancement is observed in the pore with 1 μm diameter around 20.8 ps.

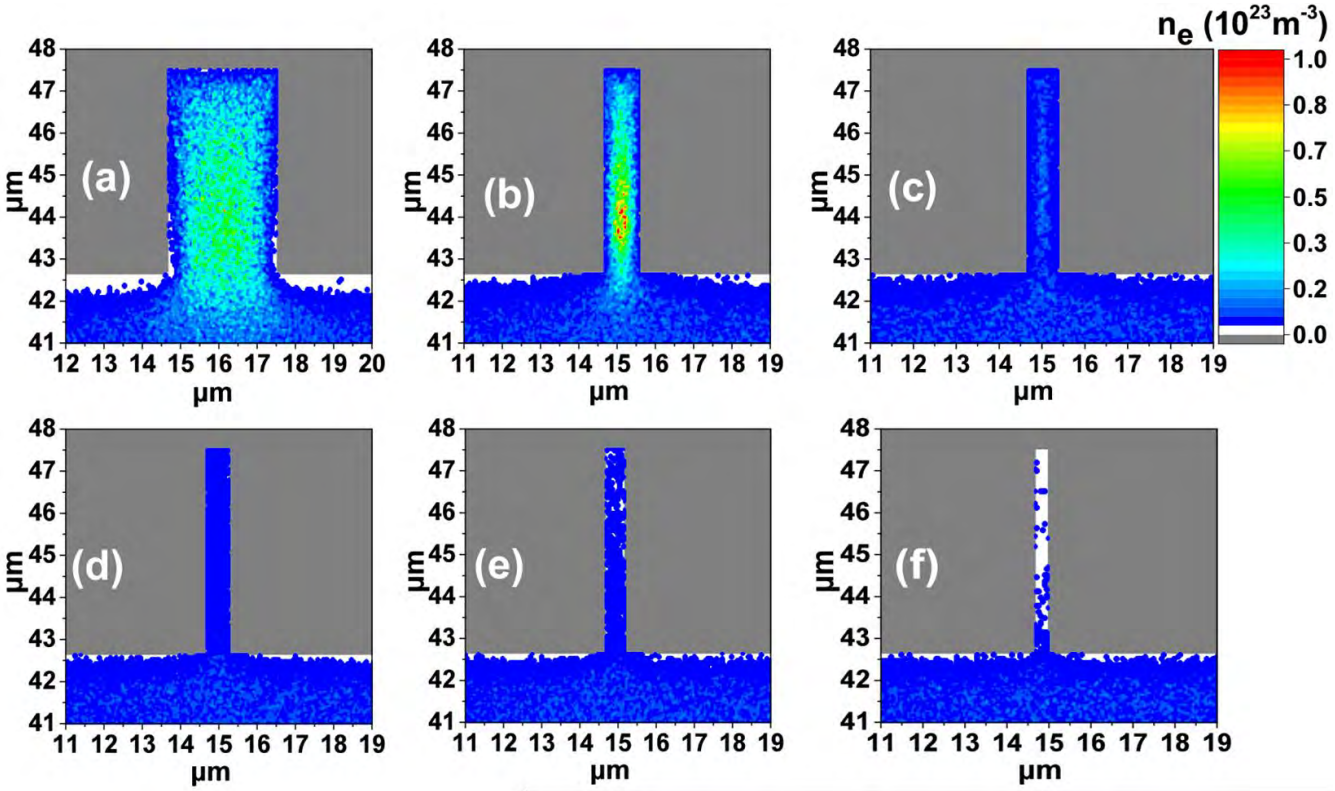

Figure 3. Plasma density distributions n_e (m^{-3}) near and inside a pore, with diameter of (a) 3 μm, (b) 1 μm, (c) 800 nm, (d) 700 nm, (e) 600 nm, (f) 400 nm, at 20.8 ps, and for an applied DC voltage of – 3 kV.

When rising the applied DC voltage to -5 kV, the average plasma density (i.e., averaged over the streamer head) in the streamer head increases to 6.8×10^{21} m^{-3}, and the electron temperature becomes ca. 32 eV in the streamer head. This induces a Debye length, λ_{de} of ≈ 510 nm, and the plasma can thus propagate into smaller diameter pores above 600 nm, and the strongest discharge enhancement appears in the 800 nm diameter pore around 17.6 ps, as shown in figure 4.

In figure 2, only a limited number of electrons could go inside the 50 nm pore before the sheath was formed, and this penetration of electrons was caused by diffusion, because the Debye length (510nm) is much larger than 50nm. On the other hand, in the present case, the pore diameter is larger than the Debye length (of 510nm), and a significant number of electrons can propagate into the pore as a streamer. Hence, in this case it is not dictated by diffusion (like in figure 2), but by streamer propagation.

When further rising the applied DC voltage to -8 kV, an even smaller Debye length of ca. 415 nm is achieved, because of the high plasma density (~1.3×10^{22} m^{-3}) and electron temperature (~40 eV) in the streamer head. Therefore, as seen in figure 5, the strongest discharge enhancement is observed in the pores with 600-800 nm diameter around 14.4 ps (cf. figure 5 (c-e)). In addition, also more electrons can be observed in a pore with 400 nm diameter than in the case of -3 kV and -5 kV (cf. figure 5(f) with figure 3(f) and 4(f)).

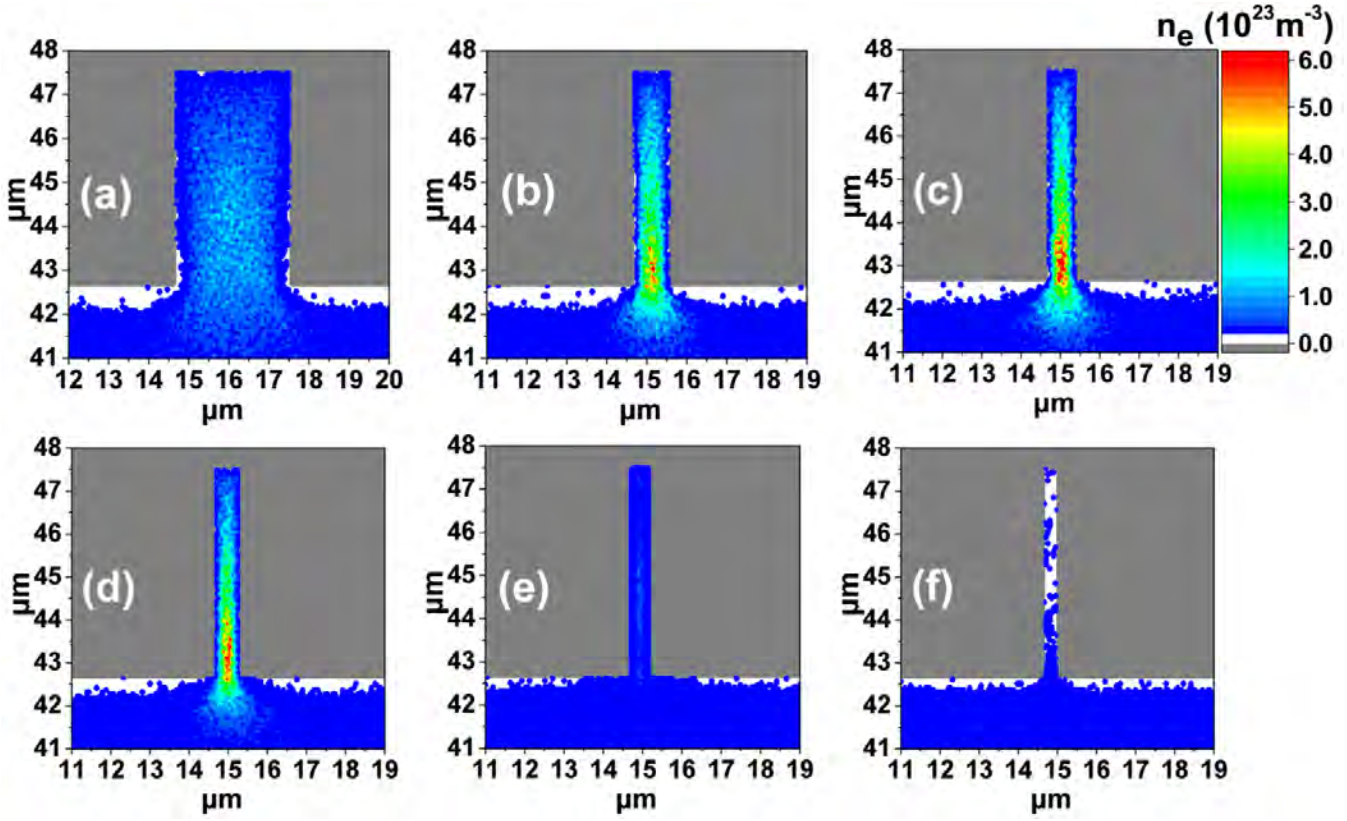

Figure 4. Plasma density distributions n_e (m^{-3}) near and inside a pore, with diameter of (a) 3 μm, (b) 1 μm, (c) 800 nm, (d) 700 nm, (e) 600 nm, (f) 400 nm, at 17.6 ps, and for an applied DC voltage of -5 kV.

Therefore, we can draw the same conclusion as Zhang et al. [16], that the Debye length is a very important criterion for plasma streamer propagation into small pores. However, our work applies to an air plasma, which is characterized by streamers, while Zhang et al. developed their model for a helium plasma in glow discharge mode. As the plasma density is much higher in the streamer head than in a helium plasma in glow discharge mode, this induces a much smaller Debye length (hundreds of nm) than the value obtained by Zhang et al. (30 μm) for a helium discharge. This indicates that plasma can penetrate into much smaller pores in a reactive air plasma (which is more often used for plasma catalysis applications) than in a helium plasma.

Figures 3-5 illustrate that a higher applied DC voltage, and consequently a stronger electric field, allows the plasma to penetrate into smaller diameter pores by increasing the density in the streamer head and thus reducing the Debye length. This is in qualitative agreement with the conclusion drawn by Hensel et al. based on their experiments [14], where the onset voltage to create micro-discharges inside catalyst pores increases with decreasing pore size. In fact, besides the applied electric field, a lot of other factors can affect the plasma density, such as material dielectric constant, pellet/bead shape and size [9, 28], and this will affect the Debye length and thus the minimum pore size into which plasma streamers can penetrate.

When the plasma streamer propagates into the pore, it interacts with the pore sidewall, yielding a significant discharge enhancement. The underlying mechanism for this is due to surface charging, which will generate an extra electric field along the pore sidewall. When this extra electric field is in the same direction as the applied electric field, the discharge will be significantly enhanced. This can be qualitatively proven by the experimental results in [9], where the plasma streamer mainly develops along the gap between the beads. In the opposite case, the two electric fields will become competitive, and there will be no discharge enhancement. More detailed explanation will be given in the next section.

We apply a strong electric field in the order between 6×10^7 V/m and 10^8 V/m. This field corresponds to real plasma catalysis conditions, for which electric fields in the range of 10^6 V/m to10^8 V/m are reported (e.g., [9, 28, 29]), to allow realistic predictions on whether plasma can propagate into catalyst pores. The strong electric field and very small simulation gap give rise to a very high electron temperature (28 ~ 40 eV) in the streamer head, i.e., much higher than the typical 7~10 eV in a DBD predicted from fluid models [16, 17, 29]. There are mainly two reasons for this. First, the newly generated electrons in the streamer head can be greatly accelerated by the local strong electric field, but they do not undergo enough collisions before they arrive at the top dielectric due to the very short distance, so they do not lose much of this energy. Actually, as seen in figure 2(a), the effective distance for the streamer to develop is only half of the discharge gap. This qualitatively corresponds to the results in [30], where the electron temperature in the streamer head is around 15 eV for a local electric field around 1.4×10^7 V/m, and the much larger electric field in our work will certainly result in a much higher electron temperature. In fact, the electron temperature will drop significantly to half its maximum value or less, after the streamer arriving at the top dielectric and forming the sheath. Second, compared to a fluid model, the electron temperature calculated from PIC simulations is generally higher, as indicated in [31]. Indeed, PIC simulations track discrete particles, which should be more accurate than fluid models, which describe the plasma species as a group, being more approximate.

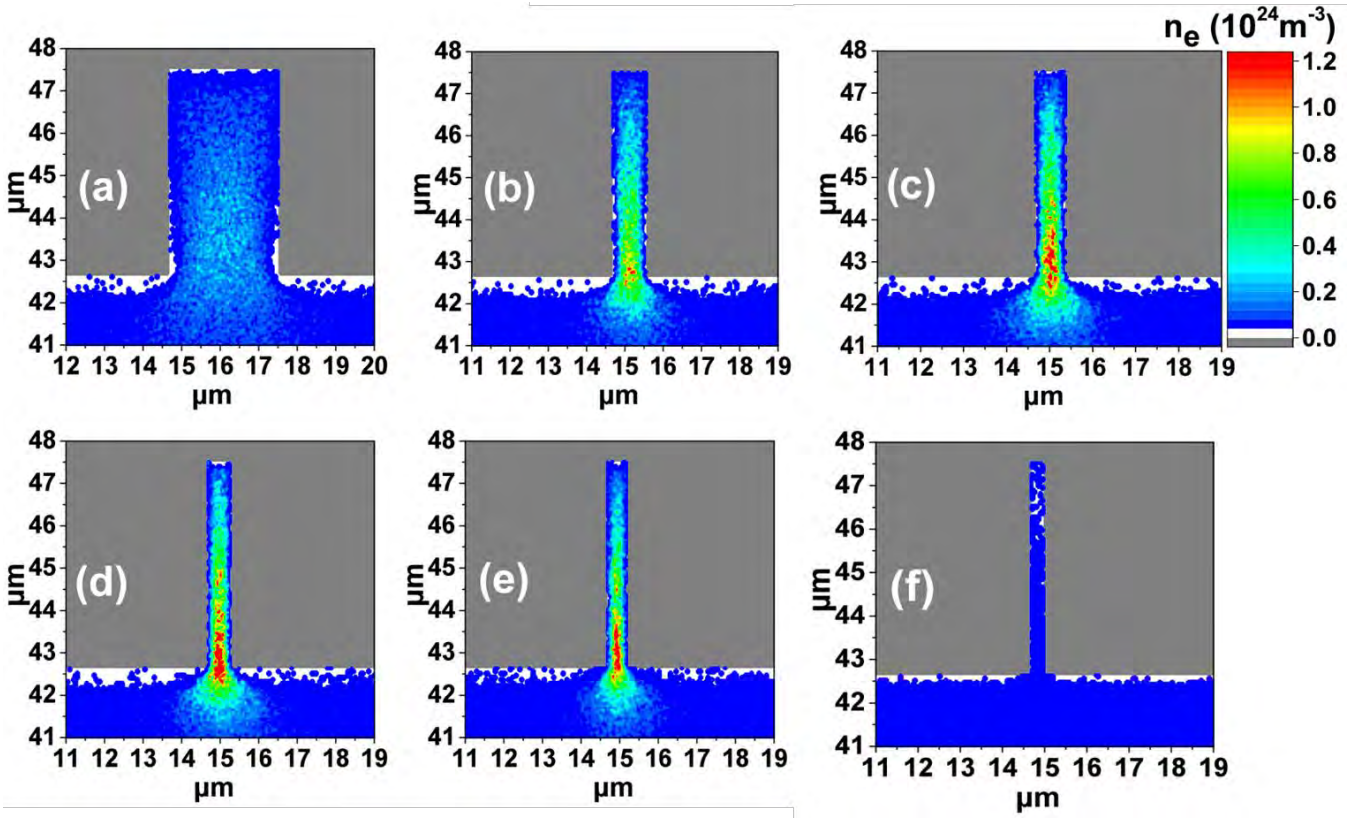

Figure 5. Plasma density distributions n_e (m^{-3}) near and inside a pore, with diameter of (a) 3 μm, (b) 1 μm, (c) 800 nm, (d) 700 nm, (e) 600 nm, (f) 400 nm, at 14.4 ps, and for an applied DC voltage of -8 kV.

3.3 Underlying mechanism of plasma streamer propagation: surface charging

Figure 6 shows the absolute surface charge density accumulated on the dielectric surface, for pores with three different diameters, at three different moments in time. Note that the surface charge density is negative, because of the much higher electron flux than positive ion flux, due to their smaller mass and thus higher velocity, but we plot the absolute value of the surface charge density. When the plasma streamer arrives at the dielectric, the electrons will charge the dielectric surface and the pore sidewalls. The charging will be non-uniform as a function of depth, as is most apparent from figure 6 (d,g), and this will induce an electric field along the surface of the pore, and thus affect the plasma discharge. For a 3 μm pore, at 8 ps the surface charging along the sidewalls is more pronounced at the pore entrance than deeper inside the pore, but the electric field induced by this surface charging points in the same direction as the applied electric field, so the total electric field is enhanced. This will further accelerate the electrons deeper inside the pore, giving rise to discharge enhancement, compared to the case with only an applied electric field. The plasma penetration in a large pore of 3 μm is quite easy, and thus the plasma streamer will reach the bottom of the pore rapidly (at 10.4 ps; cf figure 6 (b)). This yields a higher negative surface charge density near the pore bottom. At the same time, the electric field caused by these surface charges along the sidewalls is in the opposite direction of the applied electric field. The total electric field is thus reduced. This means that the discharge enhancement along the pore sidewalls only happens within a short time (up to 10.4 ps) in the 3 μm diameter pore. It is worth to note that although the electric field caused by charge accumulation at the bottom repels electrons at 10.4 ps, there is still the applied electric field, and the total electric field can still accelerate the plasma to the bottom. That is why the surface charge density in figure 6(c) at 14.4 ps is higher than in figure 6(b) at 10.4 ps.

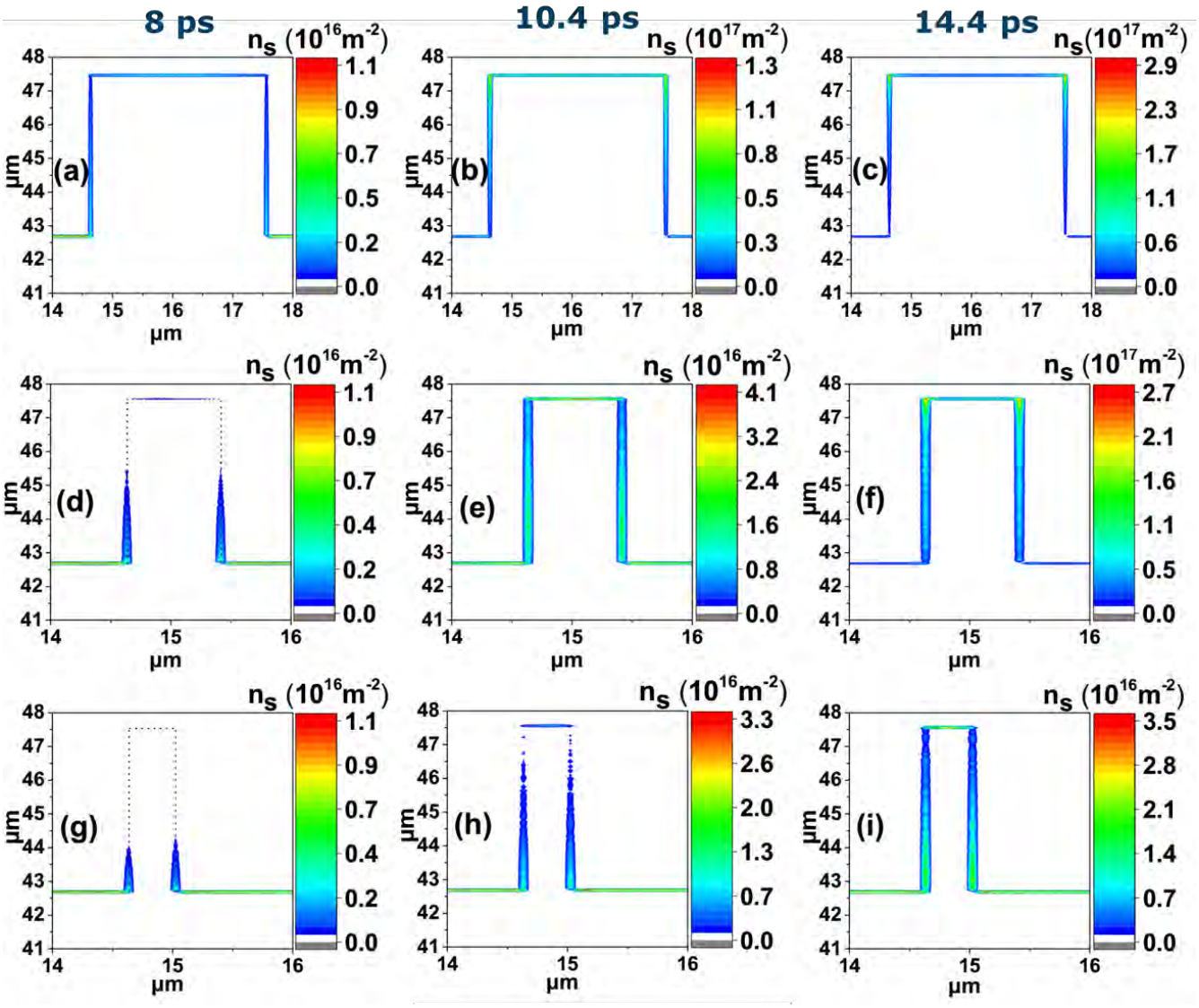

Figure 6. Absolute surface charge density n_s (m^{-2}) accumulated on the dielectric surface, near and inside a pore with diameter of 3 μm (a,b,c), 800 nm (d,e,f) and 400 nm (g,h,i), for an applied DC voltage of – 8 kV. (a,d,g – 8 ps; b,e,h – 10.4 ps; c,f,i – 14.4 ps). The black dotted line indicates the pore profile.

In contrast, it is much more difficult for the plasma to penetrate into a small pore of 400 nm. As seen in figure 6 (g,h,i), the surface charge density along the pore sidewalls remains the highest at the pore entrance up till 14.4 ps, and thus the electric field caused by surface charging can keep accelerating the electrons toward the pore bottom all the time. However, as the number of electrons that can penetrate inside a 400 nm pore, and which behave as seed electrons for plasma streamer formation, is quite limited, this significantly limits the discharge enhancement, as observed in figure 5(f).

For an intermediate pore diameter of 800 nm, the electric field caused by the non-uniform surface charging can enhance the discharge within the pore for a relatively longer time, since the surface charge density is still the highest near the pore entrance at 10.4 ps, as shown in figure 6 (d-f), and at the same time, there are abundant electrons inside the pore, which can be accelerated toward the pore bottom as seed electrons, because the Debye length is smaller than 800 nm at this applied

voltage of – 8 kV (see above). This explains why the discharge enhancement is most pronounced (cf. highest plasma density inside the pore) for a pore with 600-800 nm diameter (cf. figure 5).

3.4 Effect of pore depth on the plasma streamer propagation

To examine the effect of pore depth on the plasma streamer propagation inside the pores, we show the plasma density distributions in figure 7 for pore depths of only 1 μm, for an applied DC voltage of – 8 kV. Note that the Debye length is the same for figure 7 and figure 5, because it is the Debye length in the streamer head when it arrives at the top dielectric, and this is the same for figure 5 and figure 7. First, similar to figure 5, there is discharge enhancement within the pores with diameter larger than 600 nm, with the strongest discharge enhancement again around 700 nm. This again confirms that the plasma streamer can propagate into the pores and give rise to an enhanced discharge for pore diameters larger than the plasma Debye length in the streamer head. Second, by comparing figure 7 and figure 5, we see that the plasma density is much reduced in figure 7. This is because the much shorter pore depth will significantly shorten the penetration time to the pore bottom, which means that the discharge enhancement due to surface charging along the sidewall (cf. figure 6) can only happen within a limited time. Indeed, the plasma density in figure 7 is only comparable to the value in figure 5 within a very short time. At later times, the plasma streamer will reach the bottom of the pore and cause a higher negative surface charge density near the pore bottom, and thus an electric field in the opposite direction of the applied electric field. The total electric field is thus reduced, and the discharge enhancement stops. Consequently, the density is much smaller in figure 7 than in figure 5 for the same pore diameter. This demonstrates again the importance of surface charging in the propagation of a plasma streamer into small pores.

Therefore, we can conclude that when the pore diameter is larger than the plasma Debye length, a higher aspect ratio of the pores will correspond to a more pronounced discharge enhancement along the pore sidewall, due to the longer propagation time before reaching the pore bottom.

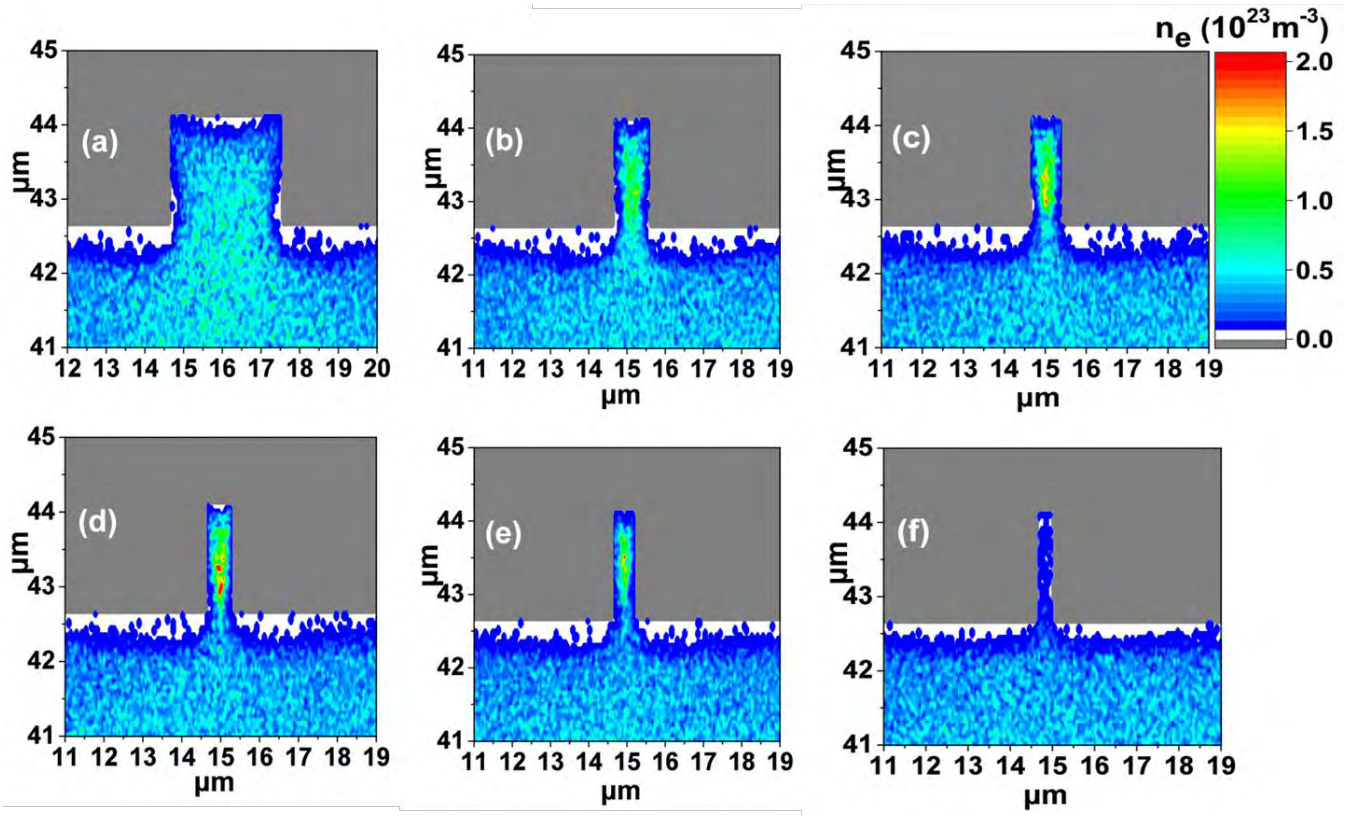

Figure 7. Plasma density distributions n_e (m^{-3}) near and inside a pore, with diameter of (a) 3 μm, (b) 1 μm, (c) 800 nm, (d) 700 nm, (e) 600 nm, (f) 400 nm, and pore depth of 1 μm, at 14.4 ps, and for an applied DC voltage of -8kV

4. Conclusions

In this paper we studied plasma streamer propagation and discharge enhancement inside catalyst pores, to be able to answer the important research question in plasma catalysis whether (and how) plasma can penetrate inside these pores, and for which pore diameters. We studied the mechanism for pore diameters ranging between 50 nm and 3 m, by means of a PIC-MCC model. For very small pores in the mesoporous range (~ 50 nm), plasma can only penetrate into the pores at very short times, i.e., at the beginning of a micro-discharge, before the plasma streamer arrives at the dielectric surface and builds up a sheath in front of the surface. The few electrons that can initially penetrate into the pores, can however further induce reactive species inside the pores, which explains the presence of short lived reactive plasma species inside small pores, as deduced from experimental measurements [10, 12].

Surface charging plays an important but opposite role in streamer propagation in small (~ 50 nm) and large (600-1000 nm) diameter pores. For small diameter pores, after the streamer reaches the dielectric, surface charges will accumulate rapidly and give rise to a significant sheath in front of the surface, which will push away the plasma bulk, and make sure that no plasma can penetrate into the pores anymore. For larger diameter pores (larger than the Debye length), the plasma penetration inside the pores will induce surface charging of the pore sidewalls, leading to further discharge enhancement, depending on pore diameter and depth.

In general, the Debye length is an important criterion for plasma penetration into catalyst pores, i.e., plasma streamers can penetrate into catalyst pores when their diameter is larger than the Debye length. The same conclusion was made in [16], but for a helium discharge in glow mode, characterized by a much large Debye length, and thus it tells us that plasma can penetrate into much smaller pores in an air discharge, characterized by a filamentary mode, than in a helium discharge, which is an importance conclusion for plasma catalysis applications.

When increasing the applied DC voltage, the enhanced plasma density will reduce the Debye length, which allows the plasma streamers to propagate into smaller diameter pores. This is in qualitative agreement with experiments [14], which reveal that the onset voltage to create micro-discharges inside catalyst pores increases with decreasing pore size. At the conditions investigated here, an applied DC voltage of -8 kV allows plasma streamers to penetrate into catalyst pores above 500 nm diameter. In addition, a higher pore aspect ratio will lead to a more pronounced discharge enhancement inside the pore, at least when the pore diameter is larger than the Debye length.

In summary, our simulations can predict the minimum pore diameter needed for plasma streamers to penetrate inside catalyst pores for given operating conditions, and they provide a deeper understanding of the propagation mechanism of streamers inside these pores, for pore diameters ranging from nm to μm.

Acknowledgments

We acknowledge financial support from the European Marie Skłodowska-Curie Individual Fellowship within H2020 (Grant Agreement 702604) and from the Fund for Scientific Research Flanders (FWO) (Excellence of Science Program; EOS ID 30505023). This work was carried out in part using the Turing HPC infrastructure at the CalcUA core facility of the Universiteit Antwerpen, a division of the Flemish Supercomputer Center VSC, funded by the Hercules Foundation, the Flemish Government (department EWI) and the University of Antwerp.

References

[1] E.C. Neyts, K. Ostrikov, M.K. Sunkara, A. Bogaerts, Chem. Rev. 115 (2015) 13408.
[2] H. H. Kim, A. Ogata, S. Futamura, Appl. Catal. B Environ. 79 (2008) 356.
[3] J. Van Durme, J. Dewulf, C. Leys, H. Van Langenhove, Appl. Catal. B Environ. 78 (2008) 324.
[4] H.L. Chen, H.M. Lee, S.H. Chen, Y. Chao, M.B. Chang, Appl. Catal. B Environ. 85 (2008) 1.
[5] B.S. Patil, N. Cherkasov, J. Lang, A.O. Ibhadon, V. Hessel, Q. Wang, Appl. Catal. B Environ. 194 (2016) 123–133
[6] J.C. Whitehead, J. Phys. D: Appl. Phys. 49 (2016) 243001.
[7] E.C. Neyts, A. Bogaerts, J. Phys. D Appl. Phys. 47 (2014) 224010.
[8] K. Van Laer, A. Bogaerts, Plasma Sources Sci. Technol. 25 (2016) 015002.
[9] W.Z. Wang, H.H. Kim, K. Van Laer, A. Bogaerts, Chem. Eng. J. 334 (2018) 2467 – 2479.
[10] F. Holzer, U. Roland, F.D. Kopinke, Appl. Catal. B Environ. 38 (2002) 163.
[11] U. Roland, F. Holzer, F.D. Kopinke, Appl. Catal. B Environ. 58 (2005) 217.
[12] U. Roland, F. Holzer, A. Poppl, F.D. Kopinke, Appl. Catal. B Environ. 58 (2005) 227.
[13] K. Hensel, S. Katsura, A. Mizuno, IEEE Trans. Plasma Sci. 33 (2005) 574.
[14] K. Hensel, V. Martisovits, Z. Machala, M. Janda, M. Lestinsky, P. Tardiveau, A. Mizuno, Plasma Process. Polym. 4 (2007) 682.
[15] K. Hensel, Eur. Phys. J. D 54 (2009) 141.
[16] Y.R. Zhang, K. Van Laer, E.C. Neyts, A. Bogaerts, Appl. Catal. B Environ. 185 (2016) 56–67.
[17] Y.R. Zhang, E.C. Neyts, A. Bogaerts, J. Phys. Chem. C 120 (2016), 25923−25934.
[18] Y. Zhang, H.Y. Wang, Y.R. Zhang and A. Bogaerts, Plasma Sources Sci. Technol. 26 (2017) 054002.
[19] H. Y. Wang, W. Jiang and Y.N. Wang, Plasma Sources Sci. Technol. 19 (2010) 045023.
[20] W. Jiang, H. Y. Wang, Z. H. Bi and Y.N. Wang, Plasma Sources Sci. Technol. 20 (2010) 035013.
[21] Retrieved on 11 June 2015 Biagi-v8.9 database www.lxcat.net
[22] M.B. Zheleznyak, A. K. Mnatsakanyan, and S. V. Sizykh, High Temp. 20 (1982) 357– 362.
[23] N.Y. Liu and V. P. Pasko, J. Geophys. Res., 109 (2004) A04301.

[24] O. Chanrion, T. Neubert, J. Comput. Phys. 227 (2008) 7222–7245.
[25] Y.D. Li, R.P. Wang, Q.G. Zhang, Y. Zhou, H.G. Wang, and C.L. Liu, IEEE Trans. Plasma Sci. 39 (2011) 0093-3813.
[26] J. Teunissen and U. Ebert, Plasma Sources Sci. Technol. 25 (2016) 044005.
[27] G. Lapenta, J. Comput. Phys. 181 (2002) 317–337.
[28] K. Van Laer, A. Bogaerts, Plasma Sources Sci. Technol. 26 (2017) 085007.
[29] D. H. Mei, X. B. Zhu, Y. L. He, J. D. Yan and X. Tu, Plasma Sources Sci. Technol. 24 (2015) 015011.
[30] C. Li, U. Eberta, and W. Hundsdorfer, J. Comput. Phys. 231 (2012) 1020–1050.
[31] T. E. Nitschke, D. B. Graves, J. Appl. Phys. 69 (1991), 8047.